C. R. Mecanique 347 (2019) 716–733

Contents lists available at ScienceDirect

Comptes Rendus Mecanique

www.sciencedirect.com

A simplified solution for piled-raft foundation analysis by using the two-phase approach

Seyed Mehdi Nasrollahi, Ehsan Seyedi Hosseininia *

Civil Engineering Department, Faculty of Engineering, Ferdowsi University of Mashhad, Iran

ARTICLE INFO

Article history:
Received 23 June 2019
Accepted 7 October 2019
Available online 31 October 2019

Keywords:
Pile-raft foundation
Two-phase model
Analytical solution
Soil–pile interaction
Settlement
Elastic form

ABSTRACT

In common practice, the pile–soil–raft interaction still remains a challenging problem in the analysis of piled-raft foundations. In the present study, a simplified analytical approach is introduced to analyze a vertically-loaded piled-raft foundation by using a developed homogenization technique called the two-phase approach. In spite of classical and simplified methods in the literature, the proposed method considers the pile–soil interaction. The other major advantage is the ability to predict the axial pile load along the pile length. The problem is solved in the domain of elasticity and simple closed-form solutions are presented for the prediction of the settlement and the pile load sharing of a piled raft as well as the pile's axial force distribution along its length. The applicability of the proposed method is validated by considering case studies and field measurements. A comparison of the results indicates that the method can be utilized safely in a proper, quick, and effective manner with the least computational effort in comparison with sophisticated numerical approaches. The raft settlement can be accurately predicted while the pile load sharing might be over/under estimated. A parametric study is also carried out to investigate the response of piled-raft foundations including the influence of the parameters of the soil and the geometric characteristics of the piles.

1. Introduction

In the last decades, a major computational challenge in geotechnical engineering has been the rational design of mat footing reinforced by pile groups, namely 'piled-raft foundation,' which has been used extensively in Asia and Europe [1]. The relatively large number of piles along with the extreme heterogeneity of the soil and the interaction effects among them makes it difficult to study the response of such a soil-structure problem by using analytical as well as numerical methods. To simulate the behavior of such complex three-dimensional foundations, different analysis methods ranging from simplified [2,3] to more rigorous analyses [4] have been developed.

As for the analysis of a piled-raft foundation, approximate closed-form solutions as a simplified method have been proposed by a number of authors [5,6], which are frequently employed in preliminary design. For instance, Poulos et al. [7] studied the response of axially-loaded piled rafts among other examples. These methods are based on the application of the well-known Mindlin's equations [8], by which, the displacement caused by a point load within a semi-infinite mass is calculated. In most simplified methods, the pile–soil interactions can not be considered. Furthermore, the distribution of

* Corresponding author.
E-mail addresses: s.m.nasrollahi@mail.um.ac.ir (S.M. Nasrollahi), eseyedi@um.ac.ir (E. Seyedi Hosseininia).

https://doi.org/10.1016/j.crme.2019.10.002
1631-0721/

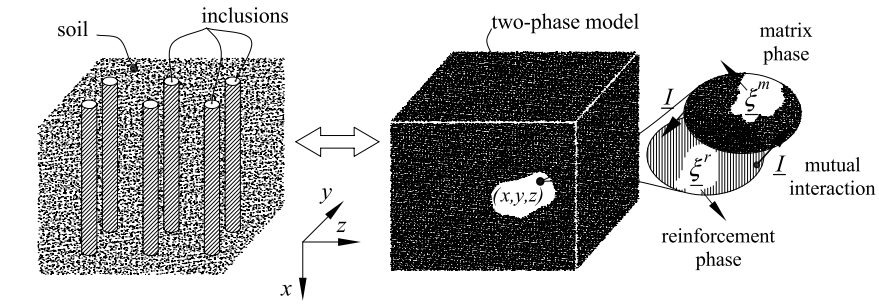

Fig. 1. Schematic representation of a pile group in the two-phase approach.

forces along the piles cannot be calculated directly. Analytical solutions can be ameliorated by applying concepts such as homogenization techniques in order to investigate more accurately the behavior of axially-loaded piled rafts embedded in soil deposits.

In a piled-raft foundation, the piles are often distributed regularly in the ground, which can be regarded as a composite system. Such a problem can be analyzed by homogenization methods, where the pile–soil region can be substituted by an equivalent anisotropic medium. The application of such a solution has already been validated for the soil improved by columnar inclusions [9]. In this approach, a composite material is replaced by a single homogeneous continuum, where the interaction between the distinct elements cannot be considered. A 'multiphase approach' as an extension of the homogenization technique has been introduced by de Buhan and Sudret [10] to overcome the shortcomings of classical homogenization methods. This approach has been used as a powerful tool to analyze reinforced soil structures such as reinforced soil retaining walls [11–13], tunnels [14,15], piled embankments [16], and strength of reinforced soils [17,18]. The multiphase approach, which is based on the principle of the virtual work, provides a mechanical framework that describes a composite material with periodically-arranged inclusions such a reinforced soil as several homogeneous media called 'phases'. The advantage of the multiphase approach is to consider the interaction among the phases. The soil and the pile group in a piled-raft foundation can be regarded as a 'two-phase system'.

In the simplest form, this concept has been used by Sudret and de Buhan [14] for the analysis of a piled-raft foundation where perfect compatibility was assumed between the displacement of the piles and the soil amongst. They demonstrated that in spite of some discrepancy in the results, the computational effort is interestingly smaller with respect to the discrete modeling of the piled-raft foundation problem, which makes parametric studies and design optimization very simple. Later on, Bennis and de Buhan [19] and afterward Hassen et al. [20] have focused on the interaction between the phases, i.e. piles and soil in piled-raft problems. The results are compared with classical numerical simulations where the piles are considered individually. General comparisons indicate that the two-phase approach yields reliable results for the estimation of settlement as well as pile force distributions. Furthermore, the interaction among the phases plays an important role. It is noted that all of these efforts were carried out numerically by the implementation of the two-phase technique into finite-element formulations.

Following the attempts in the analysis of piled-raft foundations as a two-phase material, the present study is devoted to the extension of an explicit analytical solution for a vertically-loaded piled raft embedded in an infinite soil layer. In this contribution, both the soil and the piles are assumed to behave as linear elastic materials, and the corresponding equilibrium equations are solved in the multiphase framework in one-dimensional form. Accordingly, the pile displacement as well as the stress distribution in the medium are obtained and expressed in terms of equations in a simple form. In addition to the simplicity of the proposed method, the major advantage against other simplified methods is to assess the distribution of axial force along the piles' length. The results are compared with other existing cases in the literature. Parametric studies on effective parameters are presented and discussed as well.

2. Mathematical formulation of the two-phase model

2.1. Resolution of the problem

Consider a pile group as a reinforced soil mass where vertical inclusions are embedded in a uniform pattern in a Cartesian x–y–z coordinate system as shown in Fig. 1. In the microscopic view, the individual piles are being paid attention to separately, as shown in Fig. 1a, while this medium can be regarded as a homogeneous but anisotropic two-phase material in a macroscopic view, as depicted in Fig. 1b. The two phases are called 'matrix phase,' as representative of the soil, and 'reinforcement phase,' representing the piles. Each point of the two-phase model has two independently kinematics, one related to the matrix phase (ξ^{m}) and the other one associated with the reinforcement phase (ξ^{r}). The internal forces of the phases are coupled with each other at the same geometric point by mutual interaction force ($\underline{I}$).

2.2. Static equilibrium of the two-phase model

Derivation of governing equations for a two-phase material is explained in detail by Sudret and de Buhan [14] where stress tensors of the phases are defined by the global form of the classical Cauchy stress tensor ($\underline{\underline{\sigma}}^{\mathrm{m}}$) for the matrix phase and the scalar stress (σ^{r}) for the reinforcement phase that behaves as an axial (tensile or compressive) one-dimensional element. By superposition of these two phases in a macroscopic scale, as shown in Fig. 1b, the body force ($\underline{I}$) is induced. The external forces consist of a body force ($\mathrm{P}^i\underline{G}^i$) and an inertial force ($\mathrm{P}^i\underline{A}^i$) of each phase, which both of them are exerted on the volume. The index i represents 'm' for the matrix phase and 'r' for the reinforcement phase. $\underline{G}^i$ represents the body force mass density, while $\underline{A}^i$ is the density of inertial forces.

De Buhan and Sudret [21] described in detail how to calculate the field equilibrium equations and boundary conditions of a two-phase system by using the first and second states of the virtual work principle. Accordingly, two sets of equations are eventuated for each phase as follows:

$$\begin{cases} \operatorname{div}\underline{\underline{\sigma}}^{\mathrm{m}} + \mathrm{P}^{\mathrm{m}}\underline{G}^{\mathrm{m}} - \mathrm{P}^{\mathrm{m}}\underline{A}^{\mathrm{m}} + \underline{I} = 0 \\ \dfrac{\partial \sigma^{\mathrm{r}}}{\partial x} + \mathrm{P}^{\mathrm{r}}\underline{G}^{\mathrm{r}} - \mathrm{P}^{\mathrm{r}}\underline{A}^{\mathrm{r}} - \underline{I} = 0 \end{cases} \tag{1}$$

where P^{m} and P^{r} are densities of the matrix and reinforcement phases, respectively.

The constitutive law of each phase can be stated in the general form as follows:

$$\begin{cases} \underline{\underline{\sigma}}^{\mathrm{m}} = \underline{\underline{\underline{\underline{E}}}}^{\mathrm{m}} : \underline{\underline{\varepsilon}}^{\mathrm{m}} \\ \sigma^{\mathrm{r}} = E^{\mathrm{r}}\varepsilon^{\mathrm{r}} \end{cases} \tag{2}$$

where $\underline{\underline{\underline{\underline{E}}}}^{\mathrm{m}}$ is the forth-order stiffness tensor of the matrix phase and E^{r} is the scalar form of stiffness of the reinforcement phase. $\underline{\underline{\varepsilon}}^{\mathrm{m}}$ is the strain tensor of the matrix phase and ε^{r} is the axial strain of the reinforcement phase. The solution to the equations of equilibrium together with the constitutive equations for each phase is completed by the corresponding stress boundary conditions.

2.3. Interaction between the phases

The interaction force ($\underline{I}$) in Eq. (1) is a volume density force. According to the second law of thermodynamics described by de Buhan and Sudret [21], the interaction force ($\underline{I}$) equals:

$$\underline{I} = \underline{\underline{C}}^{I} \cdot \Delta\underline{\xi} \tag{3}$$

where $\underline{\underline{C}}^{I}$ is an interaction stiffness coefficient tensor and $\Delta\xi = \xi^{\mathrm{r}} - \xi^{\mathrm{m}}$ is the relative displacement between the reinforcement and matrix phases at each geometrical point.

As for the simplest case, it can be assumed that there is no relative displacement between the phases, which is called the 'perfect-bonding' situation. This particular condition exists if the kinematics of the matrix and reinforcement phases remain identical ($\xi^{\mathrm{r}} = \xi^{\mathrm{m}}$). Alternatively, this case can be reached by defining $\underline{\underline{C}}^{I}$ as infinity in Eq. (3) [15]. The applicability of such assumption, i.e. perfect bonding, can be considered for the analysis of reinforced soil walls [11,12,22,23], since the average displacement of reinforced elements (such geogrids, etc.) can be assumed to be equal to that of the surrounding soil. For a piled-raft foundation as a two-phase material, however, the perfect bonding assumption would not be correct since the matrix (as the soil) and the reinforcement (as the piles) phase can have separate fields of displacement. It has been shown in many studies [15,19] that the interaction plays an important role in the piled raft response, and it is recommended to take it into consideration.

3. Problem solving

3.1. Definitions and assumptions

The geometric details of the problem are described in Fig. 2. Consider a piled-raft foundation over a uniform soil layer that supports a superstructure as shown in Fig. 2(a). The foundation contains an $A \times B$ rigid raft in plan founded at depth D_{f} below the ground surface, overlaying the soil mass reinforced by a group of vertical piles with length L. The cross-section area of the piles is a solid circle with the diameter d. The piles are arranged regularly and the distance between the two adjacent piles is characterized by s. The piled-raft foundation has a uniform settlement (δ) at the base level of the raft.

In order to analyze this problem by using the two-phase approach, the reinforced zone is substituted by a two-phase material with the same length L according to Fig. 2b. The building load together with the raft weight (Q) is applied at the top of the two-phase zone. The estimated settlement (δ) is identical for both matrix and reinforcement phases at $x = 0$. For simplicity, it is assumed that the raft, as well as the two-phase zone has an identical area with an equivalent radius (r_{g}). The average vertical stress applied to the soil at the level of the toe of the pile group can be estimated by distributing

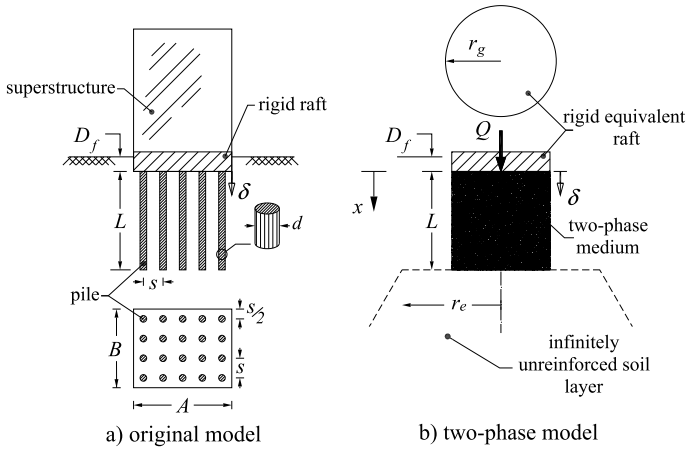

Fig. 2. Geometrical description of the problem.

the overall applied load over the extended area with radius r_e suggested by Fleming et al. [24]. Such simplification in the geometry eventuates to have a one-dimensional problem.

The phases are assumed to behave as a linear elastic material. According to Timoshenko [25], in an elastic material, radial and tangential strains are very small compared with the axial strains and, consequently, the radial deformation is ignored in this problem. Furthermore, the shear and flexural effects of the piles are disregarded in the reinforcement phase, since the loading of the piled raft is solely vertical. It is noted that, although the shear and flexural behavior of the piles can be implemented in the framework of the two-phase approach [21], Hassen et al. [26] indicated that this simplification under vertical loading has an inconsequential role in the amount of settlement of piled-raft foundations. Considerably, this assumption helps to simplify the formulation and boundary conditions of the problem.

3.2. Outline procedure

In view of the above descriptions, the equilibrium and constitutive equations of the one-dimensional elastic two-phase model are summarized in Eqs. (4) and (5), respectively, as follows:

$$\begin{cases} \dfrac{\mathrm{d}}{\mathrm{d}x}\sigma_x^{\mathrm{m}} + I_x = 0 \\ \dfrac{\mathrm{d}}{\mathrm{d}x}\sigma_x^{\mathrm{r}} - I_x = 0 \end{cases} \tag{4}$$

$$\begin{cases} \sigma_x^{\mathrm{m}} = E^{\mathrm{m}}\left(\dfrac{\mathrm{d}}{\mathrm{d}x}w_x^{\mathrm{m}}\right) \\ \sigma_x^{\mathrm{r}} = E^{\mathrm{r}}\left(\dfrac{\mathrm{d}}{\mathrm{d}x}w_x^{\mathrm{r}}\right) \end{cases} \tag{5}$$

where σ_x^{r} and σ_x^{m} are the phase stresses and w_x^{r} and w_x^{m} indicate the vertical displacement related to the reinforcement and matrix phases at an arbitrary depth x, respectively.

In the context of a one-dimensional elastic behavior, the interaction body force density ($\underline{I}$) is reduced to one single component along the pile direction:

$$I_x = C^I\left(w_x^{\mathrm{r}} - w_x^{\mathrm{m}}\right) \tag{6}$$

A general view of the one-dimensional two-phase model and the boundary conditions of both reinforcement and matrix phases are sketched, separately, in Fig. 3. The simplified model of the problem is shown in Fig. 3a, in which the piled zone is substituted by a two-phase material. The details of the boundary conditions are figured in Fig. 3b. The top boundary of the zone, where the equivalent raft is located ($x = 0$), has the same displacement (δ) in each phase. The sum of matrix and reinforcement stresses at this boundary equals the average imposed pressure $q = Q/(A \times B)$. The other boundary condition that prescribes a pile-toe reaction is imposed at the lower surface of the zone ($x = L$). For each phase:

$$\begin{cases} \sigma_{x=L}^{\mathrm{m}} = -q + p \\ \sigma_{x=L}^{\mathrm{r}} = -p \end{cases} \tag{7}$$

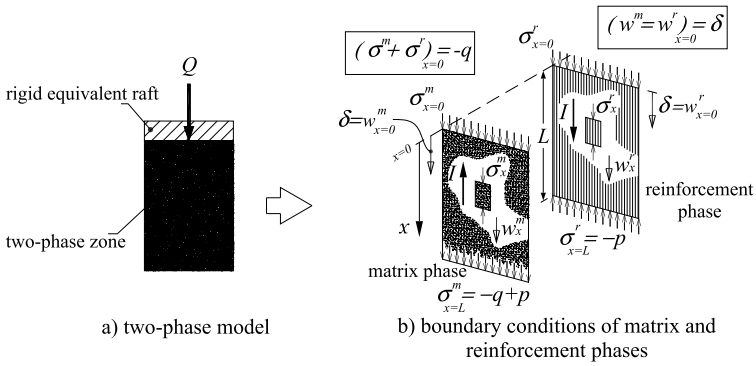

Fig. 3. Schematic view of the basic assumptions and boundary conditions of the problem.

where p is the axial stress caused by the interaction between the phases at the pile toe at the macroscopic scale. This stress, which corresponds to the pile force at the pile toe, is exerted on the lower boundary of reinforcement phase with the positive sign and reciprocally in the matrix phase with the negative sign, as shown in Fig. 3b.

By replacing the interaction volume density I_x (Eq. (6)) and the constitutive equations (Eq. (5)) in the equilibrium equations (Eq. (4)) of the system, the final set of differential equations in the two-phase material is obtained:

$$\begin{cases} E^{\mathrm{m}} \dfrac{\mathrm{d}^2}{\mathrm{d}x^2} w_x^{\mathrm{m}} + C^I \left(w_x^{\mathrm{r}} - w_x^{\mathrm{m}} \right) = 0 \\ E^{\mathrm{r}} \dfrac{\mathrm{d}^2}{\mathrm{d}x^2} w_x^{\mathrm{r}} - C^I \left(w_x^{\mathrm{r}} - w_x^{\mathrm{m}} \right) = 0 \end{cases} \tag{8}$$

By introducing the relative displacement of the reinforcement and matrix phases $\Delta(x) = w_x^{\mathrm{r}} - w_x^{\mathrm{m}}$, Eq. (8) simplifies to:

$$\frac{\mathrm{d}^2}{\mathrm{d}x^2}\left[\Delta(x)\right] - \frac{1}{\lambda^2}\Delta(x) = 0 \tag{9}$$

where $\lambda = \sqrt{\frac{E^{\mathrm{m}} E^{\mathrm{r}}}{C^I (E^{\mathrm{m}} + E^{\mathrm{r}})}}$ is named as characteristic length.

The general solution of Eq. (9) is in the form:

$$\Delta(x) = c_2 \sinh\left(\frac{x}{\lambda}\right) + c_1 \cosh\left(\frac{x}{\lambda}\right) \tag{10}$$

The constant c_1 in the above equation is 0 because the boundary condition ($w_{x=0}^{\mathrm{r}} = w_{x=0}^{\mathrm{m}} = \delta$) is accepted at the top of the two-phase zone ($x = 0$). The constant c_2 is obtained from the lower boundary condition.

Substitution of Eq. (7) into Eq. (5) at $x = L$ leads to the following differential equation:

$$\left[\frac{\mathrm{d}}{\mathrm{d}x}\Delta(x)\right]_{x=L} = \frac{q}{E^{\mathrm{m}}} - p\left(\frac{1}{E^{\mathrm{m}}} + \frac{1}{E^{\mathrm{r}}}\right) \tag{11}$$

In order to solve the differential equation above, it is assumed that $p = 0$, which means that the piles totally transfer the load to the surrounding soil through side friction and that the pile toe carries no load. In order to justify this simplification, it is reminded that, based on the results of Reese and O'Neill's work [27], the full friction of the drilled piles is generally mobilized at very smaller pile displacement in comparison to the pile toe and so, the pile can be regarded as a "floating pile". In the literature review, there are many examples indicating that the load proportion of the pile toe is small in slender piles [28–30]. For instance, by comparing the results of in situ measurement with those of numerical simulations, Fleming et al. [24] showed that the load proportion of a pile with a diameter of 0.8 m, a length of 20 m, and situated in a uniform soil layer is less than 10%. Poulos and Davis [28] analytically demonstrated that the pile toe carries less than 10% if the ratio of the pile diameter to the pile length is less than 0.1. Basile [29] concluded a similar result by studying numerically the nonlinear behavior of vertically loaded piled rafts. Based on detailed in situ measurements, Yamashita [30] and Yamashita et al. [31] reported a very small portion of pile toe load (less than 7%) for a 47-story building constructed over a piled raft that was installed in sand and gravel layers. These examples show that the floating piles carry non-zero but very small ratio of total load at their toe. It should be noted that in the framework of the two-phase model as a numerical approach, it is possible to implement a pile–soil interaction law as the pile toe resistance [32]. However, for more simplicity, the pile-toe load is ignored in the present analytical approach. By assuming that $p = 0$, Eq. (11) simplifies to:

$$\left[\frac{\mathrm{d}}{\mathrm{d}x}\Delta(x)\right]_{x=L} = \frac{q}{E^{\mathrm{m}}} \tag{12}$$

The term in the bracket can be obtained from the derivative of Eq. (10) and can be replaced into Eq. (12) with $x = L$ to determine the constant c_2:

$$c_2 = \frac{q\lambda}{E^{\mathrm{m}}}\left(\frac{1}{\cosh(\frac{L}{\lambda})}\right) \tag{13}$$

and consequently:

$$\Delta(x) = \frac{q\lambda}{E^{\mathrm{m}}}\left(\frac{\sinh(\frac{x}{\lambda})}{\cosh(\frac{L}{\lambda})}\right) \tag{14}$$

By integrating the equilibrium equations (Eq. (4)) and considering Eq. (14) and the stresses $\sigma^{\mathrm{r}}_{x=L}$ and $\sigma^{\mathrm{m}}_{x=L}$ from boundary conditions (refer to Fig. 3), the stress distribution in the reinforcement and the matrix phases can be calculated, respectively, by using Eqs. (15) as follows:

$$\begin{cases} \sigma^{\mathrm{r}}(x) = -\dfrac{qE^{\mathrm{r}}}{E^{\mathrm{m}}+E^{\mathrm{r}}}\left(1-\dfrac{\cosh(\frac{x}{\lambda})}{\cosh(\frac{L}{\lambda})}\right) \\ \sigma^{\mathrm{m}}(x) = -\dfrac{q}{E^{\mathrm{m}}+E^{\mathrm{r}}}\left(E^{\mathrm{m}}+E^{\mathrm{r}}\dfrac{\cosh(\frac{x}{\lambda})}{\cosh(\frac{L}{\lambda})}\right) \end{cases} \tag{15}$$

The displacement profile of the reinforcement and matrix phases is determined by considering the integration of the constitutive equations (Eq. (5)) and phase stress components (Eq. (15)) as well as the boundary condition at the ground surface ($w^{\mathrm{r}}_{x=0} = w^{\mathrm{m}}_{x=0} = \delta$):

$$\begin{cases} w^{\mathrm{r}}(x) = -\dfrac{q}{E^{\mathrm{m}}+E^{\mathrm{r}}}\left(x-\dfrac{\lambda\sinh(\frac{x}{\lambda})}{\cosh(\frac{L}{\lambda})}\right)+\delta \\ w^{\mathrm{m}}(x) = -\dfrac{q}{E^{\mathrm{m}}+E^{\mathrm{r}}}\left(x+\lambda\dfrac{E^{\mathrm{r}}}{E^{\mathrm{m}}}\dfrac{\sinh(\frac{x}{\lambda})}{\cosh(\frac{L}{\lambda})}\right)+\delta \end{cases} \tag{16}$$

In order to find δ, the compatibility of the displacement at the boundary of the reinforced zone and the soil underneath (at $x = L$) is utilized. The settlement induced at the level of the base of the pile group can be estimated by taking the overall applied load and distributing it over the equivalent area of the pile group by radius r_{e} [24]:

$$r_{\mathrm{e}} = 2.5L_1\rho(1-\nu)+r_{\mathrm{g}} \tag{17}$$

where L_1 is the distance between the pile base and the ground surface ($= L + D_{\mathrm{f}}$). ρ is the degree of soil homogeneity and is defined as the ratio of the shear moduli at the pile mid-depth and the pile base. The settlement of the unreinforced soil layer beneath the pile group (w_{u}) can be calculated as:

$$w_{\mathrm{u}} = \frac{2Q(1-\nu_s^2)}{\pi r_{\mathrm{e}} E_{\mathrm{s}}} \tag{18}$$

where E_{s} and ν_{s} are the elastic properties of the unreinforced soil beneath the piled raft whose values correspond to the toe level of the piles. The compatibility requirement between the displacements of the matrix phase ($w^{\mathrm{m}}_{x=L}$) and w_u leads to calculate δ as a final result:

$$\delta = \frac{q}{E^{\mathrm{m}}+E^{\mathrm{r}}}\left(L+\lambda\frac{E^{\mathrm{r}}}{E^{\mathrm{m}}}\tanh\left(\frac{L}{\lambda}\right)\right)+\frac{2Q(1-\nu_s^2)}{\pi r_{\mathrm{e}} E_{\mathrm{s}}} \tag{19}$$

According to Eq. (19), the total settlement of the piled-raft foundation can be assessed by two sentences. The first one shows the settlement contribution of the two-phase medium and the second sentence represents the additional settlement caused by the soil layers beneath the pile group. The soil stiffness in the two-phase medium (E^{m}) is assumed to be constant and equal to the average value along the length of the pile, while the variation of the soil stiffness beneath the piled-raft foundation is considered in the second sentence by the parameter r_{e} according to Eq. (17).

3.3. Identification of the two-phase model parameters

Application of the two-phase approach to analyze a piled-raft foundation introduces new parameters, including E^{m}, ν^{m}, E^{r}, and C^I, which can be estimated mechanically and geometrically from the characteristics of the soil and of the piles. In a two-phase material, the volume fraction of the soil against the piles is very large; hence, the parameters of the matrix phase (E^{m}, ν^{m}) can be assumed equal to those of the soil itself. The elastic stiffness of the reinforcement phase (E^{r}) is simply defined as the multiplication of the stiffness of a single pile (E_{pile}) by the 'reinforcement fraction' η:

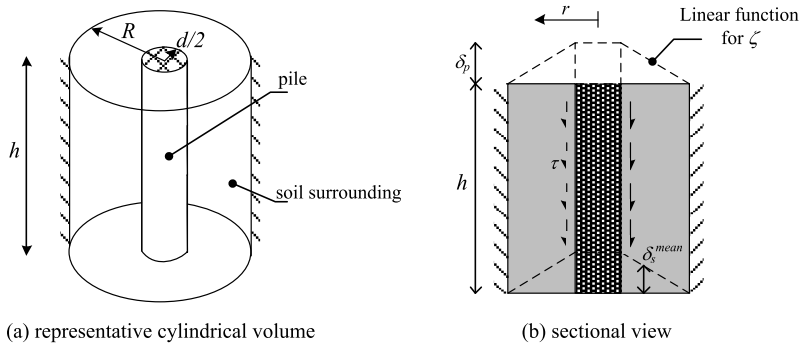

(a) representative cylindrical volume (b) sectional view

Fig. 4. View of the interaction in the RVE.

$$\eta = \frac{\pi d^2/4}{s^2} \tag{20}$$

The interaction stiffness coefficient (C^I) is a constant factor that can be determined from analytical or numerical methods based on the definition of a laterally constrained Representative Volume Element (RVE). RVE is interpreted as the smallest volume of the reinforced material, by which the corresponding calculations give a representative value of the whole. The evaluation of this coefficient has been discussed by Bourgeois et al. [32] by using finite-element simulations. In the present configuration, the value of C^I is calculated analytically based on a shape function for the deformation of a single pile in RVE, as shown in Fig. 4. The interaction stiffness coefficient is obtained from the elastic solution of an RVE with a circular cross-section (Fig. 4a), which is imposed by a predefined uniform longitudinal displacement (δ_p) to the pile. For example, as mentioned in Fig. 4b, a linear shape function (ζ) is assumed in the form of $\zeta(r) = ((R-r)/(R-0.5d))\,\delta_p$, where r is the radial distance from the center of the pile and R denotes the equivalent RVE radius ($= s/\sqrt{\pi}$). The soil around a pile shaft can be idealized as concentric cylinders in shear [33] and, consequently, the imposed shear stress around the soil is $\tau(r) = -G_s(\partial\zeta/\partial r) = G_s\left(2\delta_p/(2R-d)\right)$, where G_s is the shear modulus of the soil and equals ($= E_s/2(1+\nu_s)$). The interaction force volume density (I) is obtained by the sum of shear stresses that are longitudinally distributed throughout the lateral surface of the pile per the volume of RVE (S_p) as follows:

$$I = \frac{\int \tau \, \mathrm{d}S_p}{\pi R^2 h} \tag{21}$$

By applying a uniform displacement δ_p on the pile longitudinally, Eq. (21) is solved simply in terms of δ_p:

$$I = \frac{2d}{R^2\,(2R-d)} G_s \delta_p \tag{22}$$

As a result, the interaction stiffness coefficient is calculated from Eq. (6) as:

$$C^I = \frac{I}{\delta_p - \delta_s^{\mathrm{mean}}} \tag{23}$$

where δ_s^{mean} is the average of the longitudinal soil displacement over RVE that can be calculated as the following function:

$$\delta_s^{\mathrm{mean}} = \frac{\int_{d/2}^{R} 2\pi r \zeta(r)\,\mathrm{d}r}{\pi\left(R^2 - (0.5d)^2\right)} = \left[1 + \frac{d}{d+2R}\right]\frac{\delta_p}{3} \tag{24}$$

Accordingly, the interaction stiffness coefficient is obtained as:

$$C^I = \frac{3\pi G_s}{s^2\left(1 - 2\frac{1-\sqrt{\eta}}{\eta-\sqrt{\eta}}\right)} \tag{25}$$

Alternatively, different shape functions can be considered for the soil deformation curve. If a logarithmic function is considered for ζ, the interaction stiffness coefficient is calculated as the following relationship [19]:

$$C^I = \frac{4\pi G_s}{s^2\left(\frac{\ln\eta}{\eta-1} - 1\right)} \tag{26}$$

According to different forms of C^I (e.g., Eqs. (25) and (26)), if the pile number increases and accordingly s reduces to small values ($s \to 0$), C^I tends to infinity, which indicates perfect bonding conditions between the matrix and the reinforcement phases. According to Pando et al. [34], a rigorous analysis such as the finite-element approach indicates that Eq. (26)

Table 1
Characteristics of the hypothetical piled-raft example by Poulos et al. [35].

Example of Poulos et al. [35]			Present model	
Soil	Pile	Raft	Two-phase material	Unreinforced soil
$E = 20$ MPa $\nu = 0.3$	$E = 30{,}000$ MPa $L = 10$ m $d = 0.5$ m $n = 15$	Area $= 60$ m^2 $D_f = 0$ m	$E^m = 20$ MPa $E^r = 1473$ MPa $C^I = 11.1$ MN/m^4 $\eta = 0.0490$	$E_s = 20$ MPa $\rho = 1$ $r_e = 20.7$ m

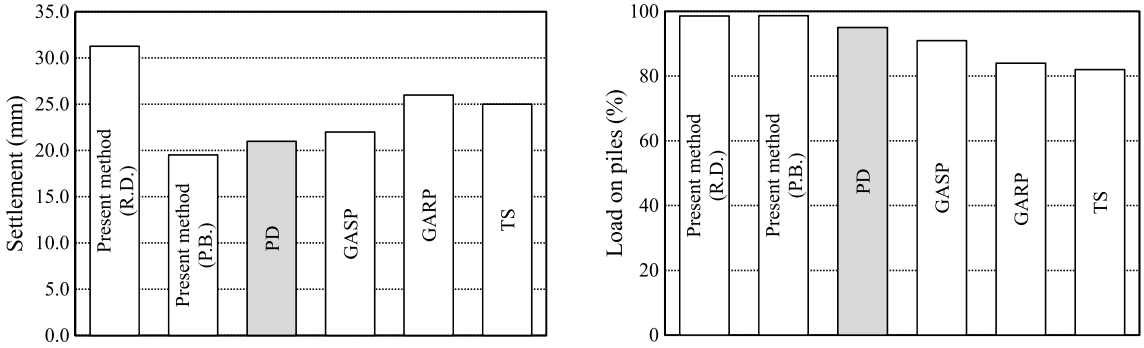

Fig. 5. Comparison of settlement and pile load sharing obtained through different methods.

is a good approximation of the deformation patterns. In this study, Eq. (26) is adopted as the definition of the interaction stiffness coefficient (C^I).

4. Validation of the proposed approach

The validity of the proposed approach is examined by considering two case studies and the results of the proposed model are compared with those of approximate solutions published in the literature.

4.1. Case study 1

The accuracy of the analytical method proposed in this paper is initially appraised by a hypothetical piled raft example presented by Poulos [7,35,36]. The piled raft contains a 6 m $\times$ 10 m raft in plan supported by 15 piles ($= 3 \times 5$) under a vertical load of 12 MN. The raft is situated on the ground surface. The piles are 10 m in length and 0.5 m in diameter. The brief collection of the data of the piled-raft model as well as the input parameters are presented in Table 1. The results of the settlement and pile load sharing are compared with alternative methods reported by Poulos [35] including Poulos and Davis' (PD) [6] approach, GARP [37] (a program based on plate on springs approach), GASP [38] (a program based on strip on springs approach), and a simplified method by Ta and Small [39], denoted hereafter by TS. It is noted that the simplified PD method is based on an elastic approach in a semi-infinite field with a perfectly-rigid or a perfectly-flexible raft, while in the GARP or GASP method, an elastic-perfectly plastic model for the soil is taken into account along with the flexibility of the raft. In the TS method, a finite layer for the soil and a finite element method for the raft and piles were considered and the slippage between the piles and soil was not regarded. According to Poulos [35], it is not possible to specify which method gives the correct answer. However, the results of different approaches should not be so far from each other. The comparison of the settlement and the proportion of load taken by the piles are illustrated in Fig. 5 for different approaches. By using the proposed method, the example has been analyzed by assuming two different conditions including:

i) the piles are perfectly bonded to the soil (denoted as P.B.);
ii) the relative displacement between the piles and the soil is considered (denoted as R.D.).

It can be seen that the results of the proposed method with PB are in good agreement with the prediction from the PD method, while other methods give larger values. In the case of RD, the piled-raft foundation behaves significantly softer than the other methods. The pile load sharing is assessed higher than the other methods which are almost the same for both interaction conditions (RD or PB) and is more similar to the PD method. The comparison of the results indicates that considering the interaction of the piles and the soil has more effect on the estimation of the settlement rather than considering the pile load sharing. The same result has been pointed out by Bourgeois et al. [32,40], who performed elaborate three-dimensional numerical analyses.

Table 2
Parameters of the piled-raft foundation investigated by Clancy et al. [41].

Example of Clancy et al. [41]			Present model	
Soil	Pile	Raft	Two-phase material	Unreinforced soil
$E = 280$ MPa $\nu = 0.4$	$E = 35000$ MPa $L = 20$ m $d = 0.8$ m $n = 81$	Area $= 1296$ m^2 $D_f = 0$ m	$E^m = 280$ MPa $E^r = 1100$ MPa $C^I = 30.5$ MN/m^4 $\eta = 0.0314$	$E_s = 280$ MPa $\rho = 1$ $r_e = 48.1$ m

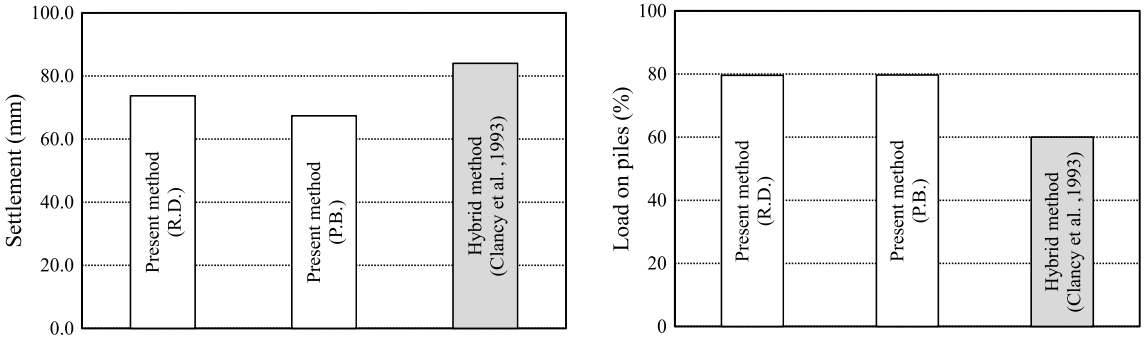

Fig. 6. Prediction of settlement and pile load percentage of a piled-raft using the present method and Clancy et al.'s [41] method.

4.2. Case study 2

An analysis is performed for a square raft supported by 9 × 9 piles under a vertical load of 1296 MN, as described by Clancy et al. [41]. It is assumed that the raft is established on the surface of the ground. The characteristics of the problem are given in Table 2. The results of the settlement and the pile load sharing were predicted by the hybrid method, in which thin bending plate finite elements and one-dimensional bar finite elements were considered for the footing and the piles, respectively. The soil response was modeled by means of springs. The settlement of the piled raft model and the pile load sharing are presented in Fig. 6 with all the aforementioned methods, as well as the proposed method. The example has been analyzed by assuming P.B. and R.D. conditions. The comparison shows that the settlement of the present method based on the relative displacement (R.D.) is more consistent with those of Hybrid method, while in the case of P.B., the settlement is underpredicted. The reason for the difference is that the piles and the soil were considered individually in the hybrid method, which can be regarded as an interaction effect between the piles and the soil. The pile load sharing calculated by the proposed method is overestimated with respect to the hybrid method, in a similar fashion to what was observed in the previous case study.

5. Case histories

To present the reliability of the approach introduced in this paper, the proposed approach is applied to analyze two published real case histories, in which a monitoring system of instrumentation was involved.

5.1. Stonebridge Park building

The first case history is the footing of a building in Stonebridge Park, London, as described firstly by Cooke et al. [42] and then investigated by other researchers [24,36]. The 16-story building was constructed from 1973 to 1975 and had one of the first instrumented piled systems to understand the proportion of carried load by the piles. The London clay layer is extended to the ground surface in the site. The foundation consists of 351 bored, cast-in-situ concrete piles with a diameter of 0.45 m and a length of 13 m. The piles are laid out in a rectangular configuration with a spacing of 1.6 m, which supports a raft with a flat surface of 20.8 m × 43.3 m and a thickness of 0.9 m. The raft was constructed at a depth of 2.5 m below the ground surface. In Table 3, a summary of the geometrical and geotechnical data is presented.

According to the observations from the instrumentation results, a total of full dead and live loads after the completion was 155.6 MN, including the weight of the raft [42]. The shear modulus profile of the site is approximated to have a linear variation with depth [24]. The elastic modulus of each pile is calculated by using the cube strength of concrete (= 25.5 MPa) and a recommended BS standard relationship [43]. Based on the available instrumented data and the results of pile loading tests, Cooke et al. [42] stated that the pile behavior was elastic.

The predicted as well as measured settlement of the piled-raft foundation from different approaches is presented in Fig. 7. Fleming et al. [24] predicted the settlement by using a simple approach with more than 10% error. By applying the proposed two-phase method, there is a very good agreement between the measured and predicted value if the interaction

Table 3
Characteristics of the foundation of the building in Stonebridge Park [42].

Measured [42]			Present model	
Soil	Pile	Raft	Two-phase material	Unreinforced soil
$G = 15.7 + 1.44\,x$ (MPa) $\nu = 0.5$	$E = 26{,}500$ MPa $L = 13$ m $d = 450$ mm $n = 351$	Area $= 900$ m^2 $D_f = 2.5$ m	$E^m = 86$ MPa $E^r = 1643$ MPa $C^I = 71.3$ MN/m^4 $\eta = 0.0620$	$E_s = 114$ MPa (at pile toe) $\rho = 0.75$ $r_e = 30.50$ m

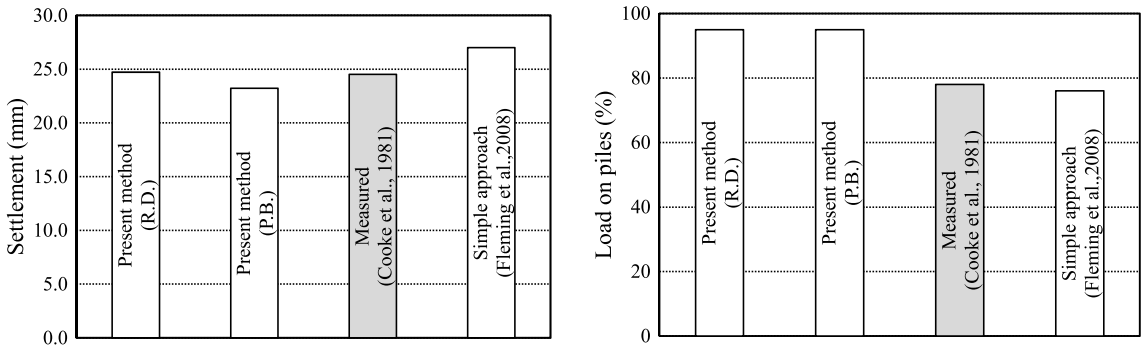

Fig. 7. Prediction of settlement as well as pile load sharing for the piled-raft of the 16-story building in Stonebridge Park.

effect (R.D. condition) is taken into account. The settlement obtained from the perfect bonding (PB) is predicted as very close to the case with the relative displacement (less than 7%). This small difference between the results can be explained by the existence of a large number of piles. Referring back to Eq. (26), as the reinforcement density increases, C^I tends to infinity, which indicates perfect bonding condition between the matrix and the reinforcement phases. Accordingly, the values of pile load sharing from the two conditions (P.B. and R.D.) are obtained as being similar to each other, which is overestimated with respect to the measured data as well as to the simple approach used by Fleming et al. [24].

5.2. Forty-seven-story Nagoya Tower

The second case is that of a piled-raft foundation consisting of 50-m-long piles that supports a 47-story residential tower in Nagoya, Japan. The field measurements were conducted on the foundation settlement and axial loads of piles were reported by Yamashita et al. [31]. The building of 162 m in height with a concrete structure was constructed between 2006 and 2009. The raft with dimensions of 30.5 m by 47 m in plan was constructed 4.3 m below the ground surface and it is supported by 36 cast-in-place concrete piles. The modulus of elasticity of the piles is evaluated by using the nominal strength of concrete (= 48 MPa) and AIJ relationship [44]. The average contact pressure under the raft due to the total load (sum of dead and live loads) is 580 kPa [45]. The shear modulus profile of the site ground as proposed by Yamashita et al. [45] showed a linear increase with depth. Table 4 presents a summary of the foundation parameters with the elastic properties of the soil [45]. The overall behavior of the piled-raft foundation remains in the elastic range because the superstructure load is far less than the ultimate bearing capacity of the foundation [46] and hence, the proposed analysis method can be reasonably applied.

The measured and predicted settlement and pile load sharing values are illustrated in Fig. 8 by applying the present method as well as a simplified method proposed by Yamashita et al. [47]. The latter method was based on considering interacting elastic springs for both the piles and the soil, and the problem was solved by using the finite-element method. The comparison of the settlements shows that the value calculated by considering the relative displacement (RD) agrees well with the measured data [31], with an error of less than 3%, while the settlement predicted by Yamashita [31] is bigger than the measured value (more than 11%). In the perfect bonding conditions (PB), the settlement is underestimated by about 16% with respect to the measurement, which evidences the importance of considering the interaction. There is almost a good accordance between the measurement and the calculations for pile load sharing. The value from the present study is underestimated by about 5%, while the predicted value by Yamashita is by 3% smaller.

5.3. Messeturm Tower

As a third case history, the applicability of the proposed method is investigated for Messeturm Tower. This case is popular and well known in the literature, since the behavior of the piles and the raft was precisely instrumented and a full monitoring program was established. The advantage of this case over the other ones is that the axial force of the piles along their length has been measured too. Messeturm Tower is a 256-m-high building which was constructed between 1988 and 1991 in Frankfurt, Germany. The building has a basement with two underground floors and 60 stories, with a

Table 4
Characteristics of the foundation of the 47-story Nagoya Tower reported by Yamashita et al. [44,45,47].

Measured			Present model	
Soil	Pile	Raft	Two-phase material	Unreinforced soil
G_{ave} = 688 MPa (at pile mid-depth) G_{ave} = 159 MPa (at pile toe) ν = 0.30	E = 36000 MPa L = 50.2 m d_{ave} = 1700 mm n = 36	Area = 1434 m^2 D_f = 4.3 m	E^m = 413 MPa E^r = 2052 MPa C^I = 24.6 MN/m^4 η = 0.057	E_s = 1790 MPa (at pile toe) ρ = 0.50 r_e = 65.4 m

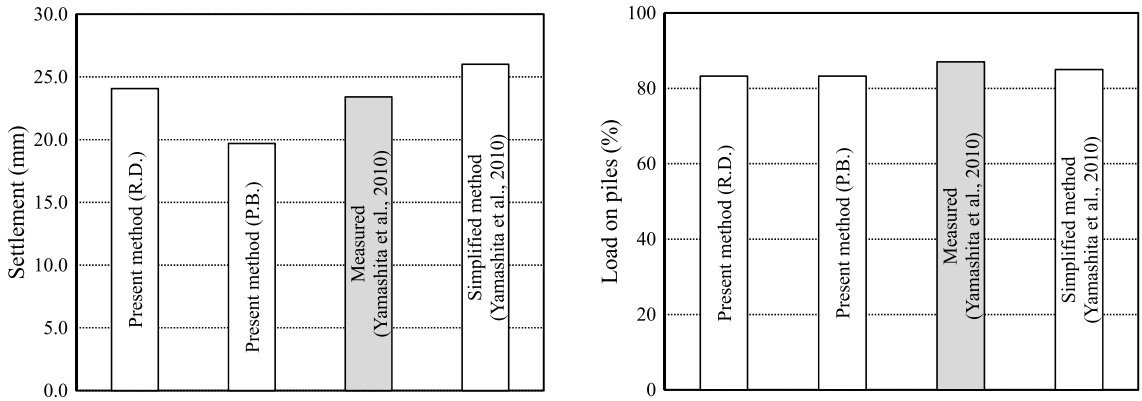

Fig. 8. Comparison of settlement and load share of the piles for 47-Story Nagoya Tower through different methods.

total estimated load of 1860 MN [48]. The foundation details are described by Sommer [49]. The 58.8-m-square raft was built at a depth of 14 m below the ground surface on overconsolidated Frankfurt clay, that was extended to a depth of more than 100 m [50]. The raft's thickness varies from 6 m at the middle to 3 m at the edge, which stands on 64 bored piles with a diameter of 1.3 m. The piles are arranged in three rings under the raft. The piles have different lengths including 26.9 m (28 piles), 30.9 m (20 piles), and 34.9 m (16 piles) in the outer, middle, and inner rings, respectively. The elastic modulus of the piles, E_{pile} = 25,000 MPa, has been derived from in-situ measurements [48]. The soil elastic modulus increases linearly with depth according to a relationship proposed by Katzenbach et al. [50]. Table 5 summarizes the parameters of the piled raft of Messeturm Tower.

The results of settlement prediction and pile load sharing obtained by the proposed method (with RD and PB conditions) are presented in Fig. 9 and compared with those of an in-situ measurement and finite-element analysis performed by Reul and Randolph [48]. According to Fig. 9a, by considering the interaction effect, the proposed method (RD) predicts the settlement very well in comparison to the measured value; however, as expected, the perfect bonding condition (PB) produces a smaller value, which highlights the role of interaction. Furthermore, the proposed method with RD gives better results than those obtained with finite element analysis. The results of the predicted pile load sharing are disappointing regardless of the soil–pile interaction conditions. The prediction error is about 50% in this case.

In order to evidence the reason for the big error observed in the predicted pile load sharing, the corresponding formulation is investigated. According to Eq. (15), the $E^r/(E^r + E^m)$ ratio plays an important role in the assessment of pile load sharing. Based on a back analysis, E^m = 350 MPa is derived and the settlement is reassessed, whose value is still satisfactory, as shown in Fig. 9b. It is noted that this high soil stiffness value is about four times the initial one calculated from the equation in Table 5 reported by Katzenbach et al. [50]. This empirical equation was derived from the back analysis of a shallow foundation, and the value was verified by Young's modulus of the soil, obtained from uniaxial compression tests. Based on the back analysis of boundary-value problems, another empirical equation was suggested by Reul and Randolph [48], whose similarly gives low values for the stiff overconsolidated Frankfurt clay. The back-calculated high value of the soil stiffness can be interpreted as the value corresponding to the small-stain level for the overconsolidated Frankfurt clay, while the reported value of the soil stiffness in the references [48,50] might correspond to large-strain problems. It is noted the authors do not intend to suggest to use small-strain soil stiffness for the analysis of piled-raft problems; however, it was only aimed to show the effect of soil stiffness on the prediction of the settlement and the pile load sharing. The selection of the soil stiffness is still a matter of debate, and an extra investigation is required in a separate work.

As mentioned before, the advantage of the proposed method is to assess the axial load distribution along the pile. In Fig. 10, the predicted axial loads of three piles in different locations beneath the raft are compared with the measured as well as finite-element analysis results performed by Sudret and de Buhan [14], Reul and Randolph[48], and Garcia et al. [51]. The calculations are based upon the characteristics of each pile (i.e. pile diameter and spacing) for inner, middle and outer rings. Figs. 10a and 10b present the results obtained by using the soil stiffness value reported in the literature [50] and that from the back-analysis (E^m = 350 MPa), respectively. The results of the analytical as well as of the numerical approaches demonstrate the same decreasing trend in the variation of the axial pile along the pile length as that of the measurement.

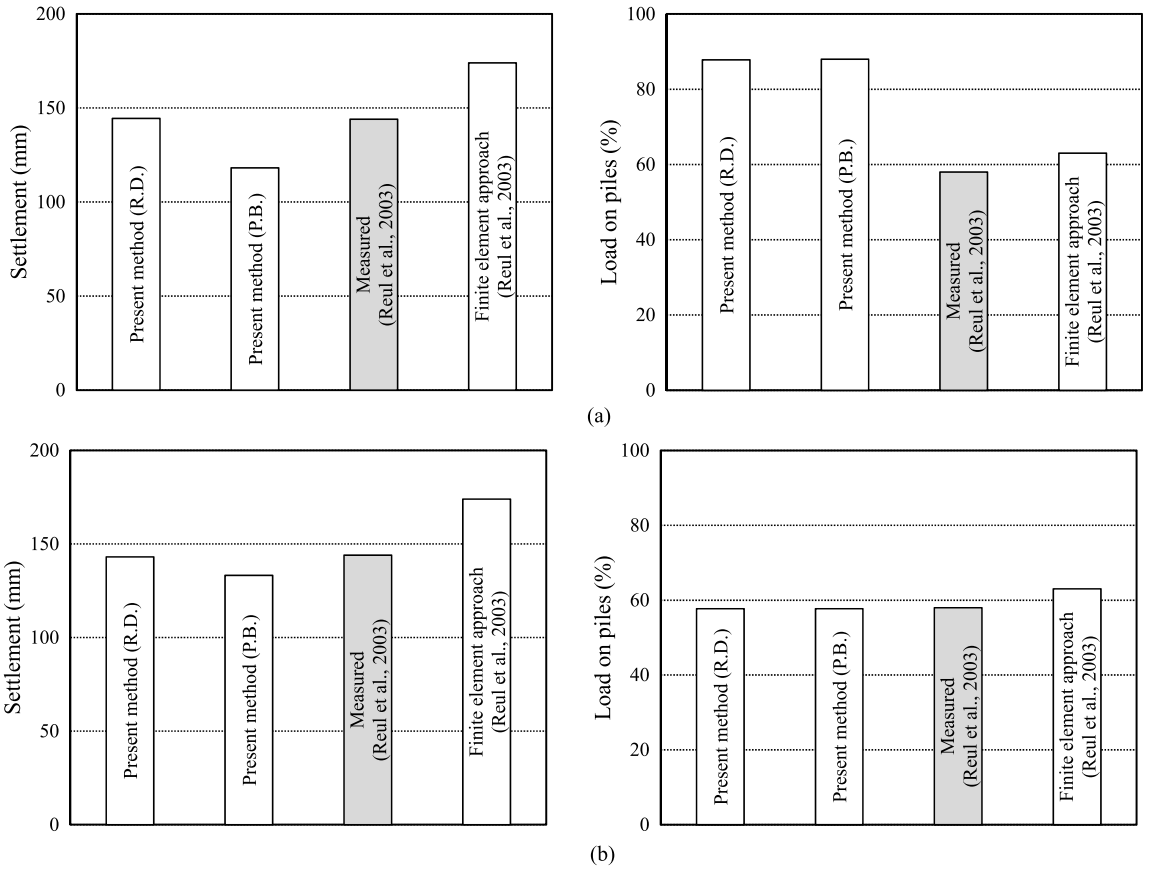

Fig. 9. Settlement and pile load sharing for Messeturm Tower predicted through different methods by using: (a) $E^{\mathrm{m}} = 84$ MPa; (b) $E^{\mathrm{m}} = 360$ MPa.

Table 5
Foundation parameters of Messeturm Tower [48–51].

Measured			Present model	
Soil	Pile	Raft	Two-phase material	Unreinforced soil
$E = 7 + 2.45\ x$ (MPa) $\nu = 0.15$	$E = 25{,}000$ MPa $L = 26.9 \sim 34.9$ m $d = 1300$ mm $n = 64$	Area $= 3457$ m^2 $D_{\mathrm{f}} = 14$ m	$E^{\mathrm{m}} = 84$ MPa (at pile mid-depth) $E^{\mathrm{r}} = 614$ MPa $C^I = 3$ MN/m^4 $\eta = 0.025$	$E_{\mathrm{s}} = 127$ MPa (at pile toe) $\rho = 0.70$ $r_{\mathrm{e}} = 101.7$ m

According to Fig. 10a, the values are discouraging for both series, especially in the lower half of the inner and middle piles. Among the numerical simulations, only the axial force of the middle pile is precisely predicted by using a rigorous finite element analysis by applying a visco-hypoplastic model [51], while for the rest of the piles, the analytical and numerical modelings have almost the same error in the prediction. As shown in Fig. 10b, the axial force of the piles is assessed smaller with respect to the previous case if a higher value of the soil stiffness is applied in the analysis. In the latter case, the axial force of the lower part of the piles is predicted with higher accuracy, while in the upper part of the piles, the values are underpredicted. Generally, it can be said that in spite of the poor quality of the prediction of the pile axial force, the present simplified method can be regarded as a proper tool for preliminary design with respect to the sophisticated finite-element approach.

By focusing on the values of pile load sharing of the case studies and the case histories mentioned above, it seems that, generally, there is no obvious difference between the results obtained from PB and R.D. conditions. To investigate this, the variation of the normalized pile load sharing in terms of $\sigma^{\mathrm{r}}_{x=0}/q\frac{E^{\mathrm{r}}}{(E^{\mathrm{m}}+E^{\mathrm{r}})}$ is calculated along with the parameter L/λ for $x = 0$, in accordance with Eq. (15). The results are presented in Fig. 11. As shown before in Section 3.3, $C^I \to \infty$ for PB, and thus, $\lambda \to 0$, which results in the infinite value of L/λ. In other words, the normalized pile load sharing is unity for PB condition. According to Fig. 11, it can be seen that the pile load sharing is sensitive for almost $L/\lambda < 5$ and reaches unity thereafter. Referring back to the previous cases, the calculation of the parameters reveals that $L/\lambda = 7.5$ and $7.4 > 5$ for the case studies 1 and 2 and $L/\lambda = 12.2, 13.4$, and $7.7 > 5$ for the following cases, respectively, and thus, the proposed

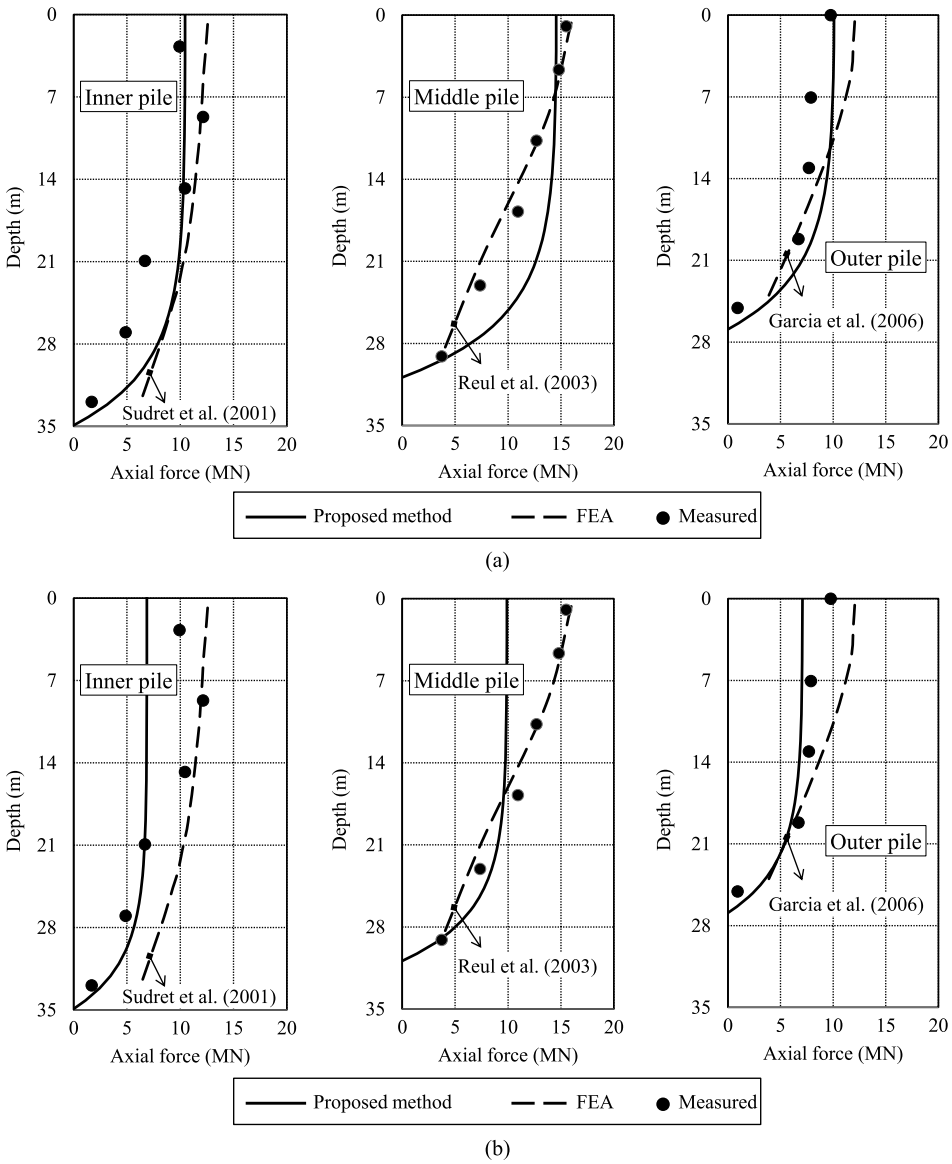

Fig. 10. Pile load distribution along the pile shaft obtained by the proposed method compared with results obtained through measurement and finite-element analysis by using: (a) $E^{m} = 84$ MPa; (b) $E^{m} = 360$ MPa.

formulation cannot allow us to distinguish pile load sharing in PB conditions from that in RD conditions. A more detailed parametric study is presented in the next section.

6. Parametric study

In this section, the proposed method is evaluated by studying the effect of significant piled raft foundation parameters on the settlement and pile load sharing. The parameters considered in the analyses are the number and the length of the piles, the raft dimensions, the elastic soil parameters and stiffness coefficient of interaction. In this parametric study, the applied load and the elastic parameters of the piles, as well as the raft, are assumed to be constant in accordance with the hypothetical example introduced by Clancy et al. [41], as already described in Section 4.2.

6.1. Pile length

In floating piles, the majority of the bearing capacity is provided by skin friction resistance, and hence the increase in pile length decreases effectively the piled raft settlement [52]. The first parametric study focuses on the influence of the length of the piles. The variation of settlement, as well as the pile load sharing of the piled raft, is shown in Fig. 12. The values

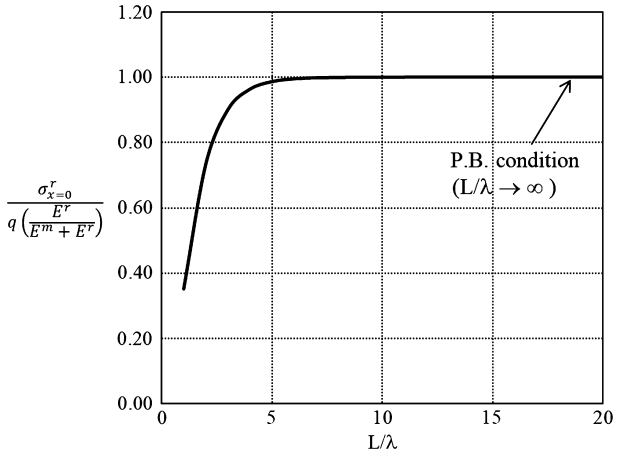

Fig. 11. Variation of normalized pile load sharing with L/λ.

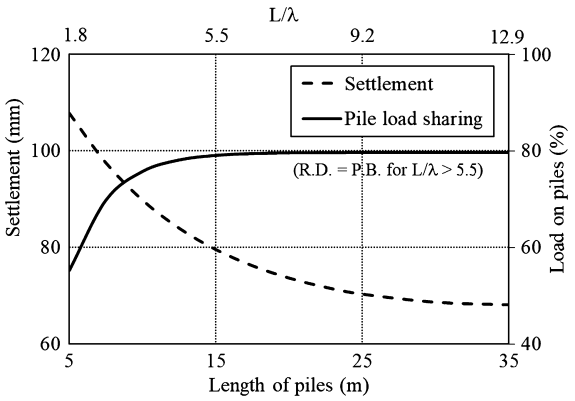

Fig. 12. Effect of pile length (and of L/λ) on the variation of settlement and pile load sharing.

of L/λ are displayed in the figure. The results show the significant influence of the length of the piles on the settlement reduction and pile load augmentation. The increase in the pile length from 5 m to 35 m causes to reduce the settlement about 36% and to increase the pile load sharing about 30%. It seems that the settlement reduces gently to a constant value at large pile length ($L \sim 30$ m). However, the value of pile load sharing is saturated sharply to a constant value ($= 80\%$) at a smaller pile length ($L \sim 15$ m). This length coincides with $L/\lambda = 5$, which was already investigated in the previous section (Fig. 11), and it was shown that, after this limit, the pile–soil interaction does not affect pile load sharing. Based on the results, the pile length has more effect on the piled raft settlement than pile load sharing.

6.2. Number of piles

To reduce the settlement of a piled raft, the increase in the pile number is commonly an effective option used in the design. However, increasing the number of piles influences the cost of the project adversely and it can lead to a non-economical design that should be carefully minimized. Fig. 13 presents the variation of the settlement of the raft and of pile load sharing with the number of piles. As expected, the settlement decreases with increasing the pile number. The settlement reduces exponentially to a limit (about 200 piles) beyond which the effect of increasing the number of piles on the settlement reduction is relatively low. A similar trend was also described in many other works in the literature [32,36, 40,53]. The number of piles has the same effect on pile load sharing, whose value increases up to an upper limit (95% approximately).In order to compare the effectiveness of the pile length with respect to the number of piles (pile spacing ratio), the piled raft settlement for a different number of piles and pile lengths are shown in Fig. 14. As already demonstrated, for a specific pile length, the settlement decreases moderately with the number of piles. It is also shown that the settlement of the raft is reduced satisfactorily when the pile length is increased from 10 m to 30 m. The comparison of the results shows that the efficiency of increasing the pile length is relatively bigger than the increase in the number of piles. For instance, if the number of piles is increased by more than three times (from $n = 81$ to $n = 256$), the reduction in the settlement (about 11%) is less than that when there is an increase of the pile length from 10 to 30 m (about 24%) by considering the same volume of the piles. It can be concluded that the pile length increase would be more efficient in reducing the piled raft settlement than the increase of the number of piles.

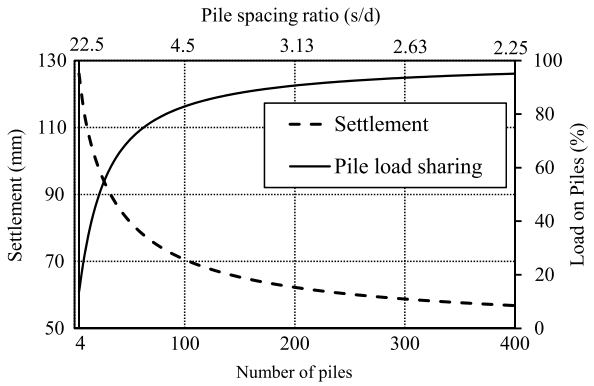

Fig. 13. Influence of the number of piles on the piled-raft settlement and pile load sharing.

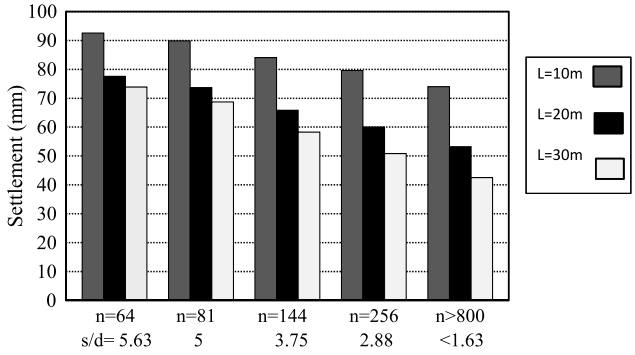

Fig. 14. Comparison of the settlement for various pile lengths and numbers.

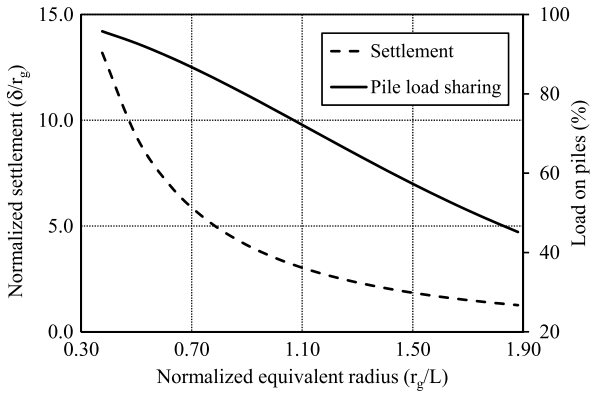

Fig. 15. Variation of the normalized settlement (δ/r_g) and pile load sharing vs. the normalized equivalent radius (r_g/L).

6.3. Raft dimensions

Logically, the increase in the dimensions of a piled raft under a constant load with a constant number of piles would lead to settlement reduction. To investigate the effect of raft dimensions on the settlement, the variation of normalized settlement (δ/r_g), as well as the pile load sharing with the normalized equivalent radius (r_g/L) of the raft, is depicted in Fig. 15. As shown, increasing r_g/L up to 1.0 reduces the normalized settlement largely, while for $r_g/L > 1.5$, the variation of the settlement is negligible. The load sharing of the piles decreases linearly with increasing the normalized equivalent radius whose reduction rate is almost constant for a wide range of values of r_g/L ($= 0.3$–1.9).

6.4. Interaction stiffness coefficient

To clarify the role of interaction stiffness, it is reminded that the interaction stiffness coefficient is affected by some mechanical and geometrical parameters, including soil shear modulus, pile diameter, and pile spacing.

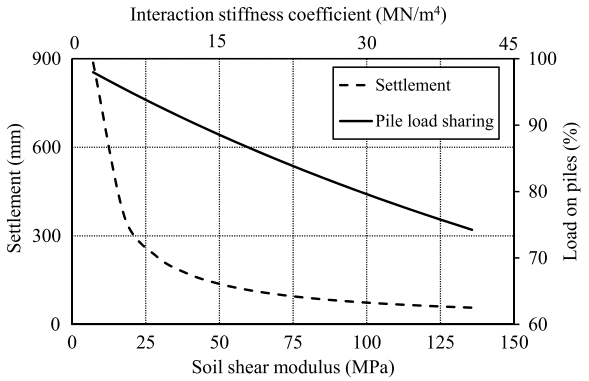

Fig. 16. Influence of soil stiffness (corresponding to C^I) on the settlement.

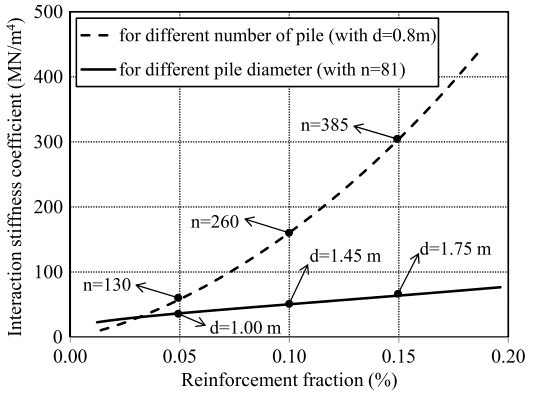

Fig. 17. Effect of the diameter and of the number of piles on the interaction stiffness coefficient.

6.4.1. Soil stiffness

The values of the settlement, as well as the pile load sharing, versus various values of the soil shear modulus G_s from 7 to 150 MPa is shown in Fig. 16 by considering constant values for other parameters. In the upper axis, the corresponding variation of C^I is also presented. The results indicate that, for softer or looser soils with $G_s < 30$ MPa (corresponding to $C^I < 10$), the settlement is decreased sharply, while for stiffer or denser soils (corresponding to C^I greater than 20), the settlement decreases gradually to a constant value. Since the increase in G_s directly influences the value of the interaction stiffness coefficient, it can be said that the pile–soil interaction resembles the perfect bonding condition. The load sharing of the piles is reduced linearly with a very gradual slope as the soil shear modulus is increased.

6.4.2. Geometrical parameters

In a piled raft, the effect of two geometric parameters, including pile spacing (s) and pile diameter (d), are reflected in the reinforcement fraction (η) according to Eq. (20). In order to compare the effectiveness of η, parametric studies are performed by considering two different cases: i) the number of piles is fixed to $n = 81$ while the diameter of the piles is varied ($d = 0.5$ to 2), and ii) the pile diameter is constant ($d = 0.8$ m) while the piles number is varied ($n = 36$ to 484). As shown in Fig. 17, the results show clearly that an increase in the number of piles has more effect on C^I with respect to the diameter of the piles with the same η. It is reminded that the effect of pile spacing has already been investigated in accordance with Fig. 13.

7. Concluding remarks

Based on the concept of two-phase model, an analytical approach is developed to analyze vertically-loaded piled-raft foundations by considering the pile–soil–raft interaction. The governing equations are derived in the domain of elasticity to predict the settlement and load sharing of the piles. The proposed method was evaluated by analytical as well as numerical analyses of different piled raft problems. The applicability and the accuracy of the proposed method were examined by measurements obtained from different case studies. Major conclusions can be drawn as follows.

- In comparison with existing analytical and numerical approaches, the proposed method can generally estimate the settlement with a good precision, although pile load sharing might be over/underpredicted. There is generally a good

agreement between the results of the proposed method and those of the field measurements. For the three case studies mentioned in this work, the settlement was predicted with acceptable accuracy, while pile load sharing was predicted with larger relative error.
- The important advantage of the proposed method is the prediction of axial load of pile along the pile length with respect to other simplified methods.

Based on the parametric studies, the analysis of a piled-raft foundation by using the proposed method shows that:

- the prediction accuracy of the settlement, as well as pile load sharing, is highly influenced by soil and pile parameters;
- an increase in the length and the number of piles reduces the settlement considerably. Among these two factors, the pile length is more efficient in the settlement reduction;
- the applicability of a piled raft highly depends on the stiffness of the soil. In the case of looser or softer soils, the piled raft can highly reduce the settlement, while it is not effective in the case of denser or stiffer soils;
- the results show that, for a constant pile volume, the interaction stiffness coefficient is more influenced by the number of piles (or, equivalently, pile spacing) with respect to the diameter of the piles diameter;
- increasing dimensions of the raft up to about twice the pile length can significantly reduce the piled-raft settlement.

In comparison with existing analytical solutions, the proposed method can properly consider the effect of soil–pile–raft interaction and it can be more easily performed in the analysis and design of piled-raft foundations against sophisticated numerical approaches. Generally, the proposed approach can give a good estimation of the settlement of piled rafts, while the load sharing of the piles might be over/underestimated. The effectiveness of the proposed method is for the problems where the applied load is in the service range and it is assumed that the soil and the piles behave elastically. In other words, the proposed method cannot capture the nonlinear behavior of piled raft in the field, since the formulation is limited to linear elasticity. However, the proposed method can be simply applied for the preliminary design of a piled-raft foundation. The proposed approach could be ameliorated in a close future in order to consider the nonlinearity in the behavior as well as the ultimate or failure state of piled-raft foundations.

References

[1] J.A. Hemsley, Design Applications of Raft Foundations, Thomas Telford, 2000.
[2] S. Jeong, J. Cho, Proposed nonlinear 3-D analytical method for piled raft foundations, Comput. Geotech. 59 (2014) 112–126.
[3] M. Huang, F. Liang, J. Jiang, A simplified nonlinear analysis method for piled raft foundation in layered soils under vertical loading, Comput. Geotech. 38 (2011) 875–882, 11//.
[4] E.M. Comodromos, M.C. Papadopoulou, I.K. Rentzeperis, Pile foundation analysis and design using experimental data and 3-D numerical analysis, Comput. Geotech. 36 (2009) 819–836.
[5] R. Butterfield, P.K. Banerjee, The problem of pile group–pile cap interaction, Géotechnique 21 (1971) 135–142.
[6] H.G. Poulos, E.H. Davis, Pile Foundation Analysis and Design, John Wiley and Sons, New York, 1980.
[7] H.G. Poulos, Methods of Analysis of Piled Raft Foundations, International Society of Soil Mechanics and Geotechnics Engineering, 2001.
[8] R.D. Mindlin, Force at a point in the interior of a semi-infinite solid, J. Appl. Phys. 7 (1936) 195–202.
[9] G. Canetta, R. Nova, A numerical method for the analysis of ground improved by columnar inclusions, Comput. Geotech. 7 (1989) 99–114, 1989/01/01/.
[10] P. de Buhan, B. Sudret, A two-phase elastoplastic model for unidirectionally-reinforced materials, Eur. J. Mech. A, Solids 18 (1999) 995–1012, 1999/11/01/.
[11] E. Seyedi Hosseininia, O. Farzaneh, Development and validation of a two-phase model for reinforced soil by considering nonlinear behavior of matrix, J. Eng. Mech. 136 (2010) 721–735.
[12] E. Seyedi Hosseininia, A. Ashjaee, Numerical simulation of two-tier geosynthetic-reinforced-soil walls using two-phase approach, Comput. Geotech. 100 (2018) 15–29, 2018/08/01/.
[13] E. Seyedi Hosseininia, O. Farzaneh, A non-linear two-phase model for reinforced soils, in: Proceedings of the ICE – Ground Improvement, vol. 164, 2011, pp. 203–211.
[14] B. Sudret, P. de Buhan, Multiphase model for inclusion-reinforced geostructures: application to rock-bolted tunnels and piled raft foundations, Int. J. Numer. Anal. Methods Geomech. 25 (2001) 155–182.
[15] P. de Buhan, E. Bourgeois, G. Hassen, Numerical simulation of bolt-supported tunnels by means of a multiphase model conceived as an improved homogenization procedure, Int. J. Numer. Anal. Methods Geomech. 32 (2008) 1597–1615.
[16] G. Hassen, D. Dias, P. de Buhan, Multiphase constitutive model for the design of piled-embankments: comparison with three-dimensional numerical simulations, Int. J. Geomech. 9 (2009) 258–266.
[17] P. de Buhan, G. Hassen, Macroscopic yield strength of reinforced soils: from homogenization theory to a multiphase approach, C. R. Mecanique 338 (2010) 132–138.
[18] G. Hassen, V.T. Nguyen, Analyse par le modèle multiphasique du comportement macroscopique de matériaux renforcés par fibres, C. R. Mecanique 340 (2012) 130–138, 2012/03/01/.
[19] M. Bennis, P. de Buhan, A multiphase constitutive model of reinforced soils accounting for soil-inclusion interaction behaviour, Math. Comput. Model. 37 (2003) 469–475, 3//.
[20] G. Hassen, P. de Buhan, B. Emmanuel, Design of piled-raft foundations by means of a multiphase model accounting for soil–pile interactions, in: COMGEO II, Croatia, 2011, pp. 704–713.
[21] P. de Buhan, B. Sudret, Micropolar multiphase model for materials reinforced by linear inclusions, Eur. J. Mech. 19 (2000) 669–687.
[22] E. Seyedi Hosseininia, O. Farzaneh, A simplified two-phase macroscopic model for reinforced soils, Geotext. Geomembr. 28 (2010) 85–92, 2010/02/01/.
[23] A. Iraji, O. Farzaneh, E. Seyedi Hosseininia, A modification to dense sand dynamic simulation capability of Pastor–Zienkiewicz–Chan model, Acta Geotech. 9 (2014) 343–353, 2014/04/01.
[24] K. Fleming, A. Weltman, M. Randolph, K. Elson, Piling Engineering, 3 ed., Taylor & Francis, 2008.
[25] S. Timoshenko, J.N. Goodier, Theory of Elasticity, 3rd edition, McGraw Hill Education (India) Private Limited, 1982.

[26] G. Hassen, P. de Buhan, A two-phase model and related numerical tool for the design of soil structures reinforced by stiff linear inclusions, Eur. J. Mech. A, Solids 24 (2005) 987–1001.
[27] L.C. Reese, M.W. O'Neil, Drilled Shafts: Construction Procedures and Design Methods, Report No. FHWA-HI-88-042, Federal Highway Administration, Washington, D.C., 1988.
[28] H.G. Poulos, E.H. Davis, The settlement behaviour of single axially loaded incompressible piles and piers, Géotechnique 18 (1968) 351–371.
[29] F. Basile, Non-linear analysis of vertically loaded piled rafts, Comput. Geotech. 63 (2015) 73–82.
[30] K. Yamashita, Field measurements on piled raft foundations in Japan, in: 9th Int. Conf. on Testing and Design Methods for Deep Foundations, Kanazawa, Japan, 2012.
[31] K. Yamashita, J. Hamada, Y. Soga, Settlement and load sharing of piled raft of a 162 m high residential tower, in: Deep Foundations and Geotechnical In Situ Testing, American Society of Civil Engineers, 2010, pp. 26–33.
[32] E. Bourgeois, P. de Buhan, G. Hassen, Settlement analysis of piled-raft foundations by means of a multiphase model accounting for soil–pile interactions, Comput. Geotech. 46 (2012) 26–38.
[33] M.F. Randolph, C.P. Wroth, Analysis of deformation of vertically loaded piles, J. Geotech. Geoenviron. Eng. 104 (1978).
[34] C.D.E. Miguel, A. Pando, George M. Filz, J.J. Lesko, E.J. Hoppe, A Laboratory and Field Study of Composite Piles for Bridge Substructures, 2006, Federal Highway Administration FHWA-HRT-04-043.
[35] H.G. Poulos, J.C. Small, L.D. Ta, J. Sinha, L. Chen, Comparison of some methods for analysis of piled rafts, in: 14th International Conference of Soil Mechanics and Foundation Engineering, Hamburg, 1997, pp. 11119–11124.
[36] H.G. Poulos, Piled raft foundations: design and applications, Geotechnique 51 (2001) 95–113.
[37] H.G. Poulos, An approximate numerical analysis of pile–raft interaction, Int. J. Numer. Anal. Methods Geomech. 18 (1994) 73–92.
[38] H.G. Poulos, Analysis of piled strip foundations, in: 7th International Conference on Computer Methods and Advances in Geomechanics, Cairns, 1991.
[39] L.D. Ta, J.C. Small, Analysis of piled raft systems in layered soil, Int. J. Numer. Anal. Methods Geomech. 20 (1996) 57–72, 1996/01/01.
[40] E. Bourgeois, G. Hassen, P. de Buhan, Finite element simulations of the behavior of piled-raft foundations using a multiphase model, Int. J. Numer. Anal. Methods Geomech. 37 (2013) 1122–1139.
[41] P. Clancy, M.F. Randolph, An approximate analysis procedure for piled raft foundations, Int. J. Numer. Anal. Methods Geomech. 17 (1993) 849–869.
[42] R.W. Cooke, D.F. Sillett, D.W.B. Smith, M.V. Gooch, Some observations of the foundation loading and settlement of a multi-Storey building on a piled raft foundation in London clay, IEE Proc. 70 (1981) 433–460.
[43] British Standard Institution, BS 8110: Structural Use of Concrete—Part 2. Code of Practice for Special Circumstances, British Standard Institution, London, 1985.
[44] Architectural Institute of Japan, Standard for Structural Calculation of Reinforced Concrete Structures, AIJ, Japan, 1985.
[45] K. Yamashita, T. Tanikawa, J. Hamada, Applicability of simple method to piled raft analysis in comparison with field measurements, Geotech. Eng. J. SEAGS & AGSSEA 64 (2015).
[46] k. Yamashita, T. Yamada, J. Hamada, Investigation of settlement and load sharing on piled rafts by monitoring full-scale structures, Soil Found. 51 (June 2011) 513–532, 2011.
[47] K. Yamashita, T. Yamada, M. Kakurai, Simplified method for analyzing piled raft foundations, in: Proceedings of the 3rd International Geotechnical Seminar on Deep Foundations on Bored and Auger Piles, Ghent, Belgium, 1998, pp. 19–21.
[48] O. Reul, M.F. Randolph, Piled rafts in overconsolidated clay: comparison of in situ measurements and numerical analyses, Géotechnique 53 (2003) 301–315.
[49] H. Sommer, Entwicklung der Hochhausgrundungen in Frankfurt, presented at the Festkolloquium 20 Jahre Grundbauinstitut, Germany, 1991.
[50] R. Katzenbach, U. Arslan, C. Moormann, Piled raft foundation projects in Germany, in: J.A. Hemsley (Ed.), Design Applications of Raft Foundation, Thomas Telford, 2000, pp. 323–391.
[51] F. Garcia, A. Lizcano, O. Reul, Viscohypoplastic model applied to the case history of piled raft foundation, in: GeoCongress 2006: Geotechnical Engineering in the Information Technology Age, Atlanta, GA, USA, 2006.
[52] S.J. Hain, I.K. Lee, The analysis of flexible raft-pile systems, Géotechnique 28 (1978) 65–83.
[53] D.D.C. Nguyen, D.S. Kim, S.B. Jo, Parametric study for optimal design of large piled raft foundations on sand, Comput. Geotech. 55 (2014) 14–26.